BMC Methods

METHODOLOGY

Open Access

Turnover rates of human muscle proteins in vivo reported in fractional, mole and absolute units

Ben N. Stansfield[1,3], Jennifer S. Barrett[1], Samuel Bennett[1,4], Connor A. Stead[1], Jamie Pugh[1], Sam O. Shepherd[1], Juliette A. Strauss[1], Julien Louis[1], Graeme L. Close[1], Paulo J. Lisboa[2] and Jatin G. Burniston[1*]

Abstract

Background Protein fractional turnover rates (FTR) represent measurements of flux through a protein pool, i.e., net abundance (ABD) of the protein. However, if protein abundance is not measured or varies between experimental conditions, the interpretation of FTR data may be confounded, potentially leading to misleading conclusions about protein dynamics. This project investigates the consequences of reporting turnover rates of human muscle proteins in vivo using mole and absolute units (which incorporate protein abundance data) compared to fractional (%/d) data, which do not account for abundance. By providing a comprehensive comparison of these metrics, we aim to refine the interpretation of protein turnover studies and offer a methodological framework for future research.

Methods Three physically active males (21 ± 1 years) were recruited and underwent a 12-day protocol of daily deuterium oxide (D_2O) consumption, with vastus lateralis biopsies collected on days 8 and 12. Protein abundances were normalized to yeast alcohol dehydrogenase, added during sample preparation, to ensure consistency across samples. Fractional turnover rates were calculated based on time-dependent changes in peptide mass isotopomer profiles. To enable a more physiologically relevant interpretation of turnover, FTR data were combined with abundance measurements (fmol/µg protein) to calculate mole turnover rates (MTR; fmol/µg protein/d) and absolute turnover rates (ATR; ng/µg protein/d), providing a more complete representation of protein kinetics.

Results Abundance data were collected for 1,772 proteins and FTR data were calculated from 3,944 peptides representing 935 proteins (average 3 peptides per protein). The median (M), lower- (Q1) and upper-quartile (Q3) values for protein FTR (%/d) were M = 4.3, Q1 = 2.52, Q3 = 7.84.

Discussion Our analyses suggest that MTR provides a more informative metric than FTR, particularly for studies investigating multiprotein complexes, where MTR accounts for potential differences in the molecular weights of component subunits. ATR may be even more advantageous than MTR and FTR, as it facilitates comparisons between samples with different abundance profiles, making it a preferred metric in conditions where protein abundance varies across experimental groups. These findings highlight the importance of incorporating protein abundance into turnover calculations to improve the biological relevance and interpretability of turnover data.

Keywords Deuterium oxide, Heavy water, Proteomics, Fractional synthesis rate, Biosynthetic labelling, Protein turnover, Skeletal muscle, Proteome dynamics, Human

*Correspondence:
Jatin G. Burniston
j.burniston@ljmu.ac.uk
Full list of author information is available at the end of the article

Introduction

In healthy adults, skeletal muscle is the largest tissue (by mass) in the human body, representing approximately 40% of total body mass and accounting for 50–70% of total body protein. Muscle proteins exist in a continuous cycle of synthesis and degradation (collectively known as protein turnover), which is essential to maintain muscle quality and facilitate changes in protein abundance profiles that underpin cellular adaptation. Losses in muscle mass are associated with heightened disease mortality [1], and changes to the turnover of muscle protein impact proteostasis and may be an important factor underpinning muscle metabolic health [2] and ageing [3]. Muscle is an accessible tissue in humans and emerging techniques for dynamic proteome profiling have the potential to offer new insight into the mechanisms underpinning human muscle adaptation [4].

The dynamic nature of proteins was established in the early 20 th Century in work led by Rudolf Schoenheimer [5], which used a stable isotope-labelled amino acid (^{15}N-tyrosine) to achieve biosynthetic labelling of newly synthesised proteins in rats in vivo. Muscle protein turnover has since been studied extensively but, for the most part, human data are constrained to reports on the average synthesis rate of mixed-protein samples based on the analysis of amino acid hydrolysates [6]. Soon after the turn of the century, advances in proteomic methods enabled studies on the turnover of large numbers of individual proteins, and were first conducted using $^{2}H_{10}$-leucine in yeast [7]. The development of stable isotope labelling of amino acids in culture (SILAC) in mammalian cells [8] enabled the turnover of individual proteins in human cell cultures using $^{2}H_{3}$-leucine. Doherty et al. [9] reports the degradation rates (K_{deg}) of almost 600 proteins in human A549 adenocarcinoma cells using dynamic SILAC with contemporary $^{13}C_{6}$-labelled lysine and arginine. Similarly, Cambridge et al. [10] used dynamic SILAC in the mouse C2 C12 muscle cell line and reported a median protein degradation rate of 1.6%/h (equating to a half-life of ~43 h) amongst 3528 proteins studied.

Dynamic SILAC requires extensive isotope labelling of amino acid precursors, which is readily achieved in cell culture and applicable in animal models but impractical in humans. Nevertheless, studies on proteome dynamics in humans are necessary to investigate complex gene-environment interactions in the context of ageing or chronic disease. Cell and animal studies are unable to capture the complexity of human tissues in vivo, and it is challenging to predict protein turnover rates in vivo from data generated in cell cultures [11]. Proteome dynamic studies in humans in vivo have investigated the turnover of individual proteins using the stable isotope, deuterium oxide (D_2O or 'heavy water'), which can be administered via a participant's drinking water. Low levels of D_2O consumption are safe and enable studies to be conducted under free-living conditions for periods of several days or more. Combined with peptide mass spectrometry (MS) D_2O labelling can be employed to measure the turnover rates of individual proteins [12], early studies in humans reported the turnover rates of specific proteins in blood [13, 14] and studies in laboratory animals have investigated proteome dynamics in, for example, liver [15, 16], heart [17, 18] and skeletal muscle [19, 20].

To our knowledge, just 5 studies [2, 4, 21–24] report dynamic proteome data in human muscle using D_2O, and mostly these works have investigated muscle responses to exercise training. In the majority, existing data on protein-specific turnover in human skeletal muscle in vivo calculate fractional synthesis rates (FSR) and report the data in percent per day (%/d) units. Amongst the previous literature, Scalzo et al. [21] reports the greatest number ($n = 381$) of proteins analysed and found deuterium incorporation was greater in male compared to female participants during a 4-weeks of sprint interval training, but numerical data on the FSR of each protein was not reported. Shankaran et al. [22] and Murphy et al. [23] provide protein-specific data on the FSR of 273 and 190 proteins, respectively, in human muscle but did not investigate the abundance of these proteins. Three earlier reports [2, 4, 24] from our laboratory include protein abundance (ABD) data alongside the measurements of protein-specific FSR in human muscle but the abundance and FSR data were not combined to report data in mole or absolute units.

Herein we use the term fractional turnover rate (FTR), which is a more suitable term than FSR when protein abundance is unchanging, and the period of isotope labelling is relatively long. Under such conditions, the rate of incorporation of label into a protein is modelled by non-linear equations that reflect the combined processes of synthesis and degradation, i.e. protein turnover. Fractional measurements (either FSR or FTR) provide information on the flux through the protein pool but are ignorant to the size of the pool (i.e. net protein abundance) and the potential inter-relationships amongst the different sizes (i.e. molecular weight; MW) and abundances of proteins. Muscle is renowned for its plasticity and can exhibit a broad repertoire of phenotypes, underpinned by different protein abundance profiles. For example, proteomic studies have highlighted robust changes to the abundance profile of proteins in human muscle in the contexts of exercise [25], ageing [26, 27] or disease [28]. Therefore, the abundance profile of muscle proteins may need to be considered alongside protein-specific turnover rate data, particularly when comparisons are made across different populations with different

muscle phenotypes. This issue has been addressed in studies in laboratory rodents [19, 29] where it is also possible to measure the total protein content of the entire muscle, which is impractical in humans. We have previously addressed this issue in vitro, by combining D_2O enrichment and yeast alcohol dehydrogenase (ADH1) spike-in, that enables the quantification of protein abundance and protein turnover in both fractional and molar units (MSR; fmol/μg total protein/day) [30]. Importantly, the biological interpretation of FSR and MSR data differed. Biological processes enriched in MSR data better represented the biological processes enriched in protein abundance data and MSR measured during early differentiation accounted for 78% of the variation in protein abundance during later differentiation, whereas FSR only accounted for 4%. These data highlight the importance of accounting for changes in protein abundance when measuring, reporting, and interpreting the biological processes associated with protein turnover measurements. Label-free proteomics data from human muscle can be normalised to spike-in standards [31] or calculated from endogenous proteins [32] to generate protein abundance data in mole or absolute (g) units expressed relative to the total amount of protein analysed, i.e. μg on column. Combined with D_2O enrichment, this allows for the measurement of protein turnover in mole and absolute units in humans in vivo. Herein, we have applied spike-in methods and D_2O enrichment to investigate for the first time the abundance and turnover rates of human muscle proteins in vivo using mole (e.g. fmol/μg total protein/day) and absolute (e.g. ng/μg total protein/day) units and we find the different units of measurement alter the biological interpretation of protein-specific turnover data in human muscle.

Methods

Participants

Three physically active males (21 ± 1 years; height 178 ± 1 cm; weight 75 ± 5 kg) were recruited and received verbal and written information, including potential risks, prior to providing written informed consent. The study was approved by the Liverpool John Moores University (LJMU) School of Sport and Exercise Science Research Committee (M18SPS006) and conformed with the Declaration of Helsinki, except registration in a publicly accessible database. Recruitment of participants began in December 2017 and the collection of data and samples from participants was completed by April 2018. All participants were recruited through internal emails and poster advertisements within LJMU.

Experimental protocol

Figure 1 provides an overview of the experimental protocol which consisted of a 12-day cross-sectional, observation study including metabolic labelling of newly synthesised protein in vivo using deuterium oxide (^2H_2O; D_2O) administration. Seventy-two hours prior to the labelling period, preparatory data including anthropological measurements (including height and weight) and peak aerobic capacity, were collected. Height was assessed using a stadiometer with a sliding headpiece, ensuring the participant stood upright with their heels, buttocks, and upper back against the vertical surface. Participants were instructed to take a deep breath and maintain a neutral head position while the headpiece was gently lowered to rest on the crown of the head. Body weight was measured using calibrated digital weighing scales, with participants standing barefoot in light clothing and maintaining a relaxed posture. Measurements were recorded to the nearest 0.1 cm for height and 0.1 kg for weight.

Baseline saliva, blood, and muscle samples were collected on day 0, prior to daily D_2O administration. Saliva and venous blood samples were collected on days 0, 4, 8 and 12 to measure body water deuterium enrichment. Muscle samples were also collected on days 8 and 12 via micro-needle biopsy of the vastus lateralis.

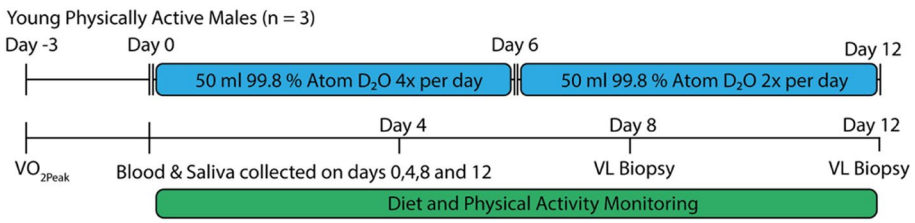

Fig. 1 Experiment design. Visual schematic of the experimental design employed in the current study. Performance measures and biometric data (outlined in Table 1) were collected 3 days prior to the study commencement. Blood and saliva were collected on days 0, 4, 8 and 12, to calculate D_2O precursor enrichment. Fifty millilitres of 99.8% D_2O was consumed by all participants 4× per day for the first 6 days. This dose was lowered to 2× per day for days 6–12. Vastus lateralis biopsies were taken on day 8 and day 12 of the experimental period. Diet and physical activity monitoring were conducted throughout the experimental period (day 0–12)

Assessment of aerobic exercise capacity

Participants attended the laboratory in the morning after an overnight fast and their resting heart rate and blood pressure were measured (DINAMAP V100, General Healthcare, UK) in a seated position. Peak oxygen uptake ($\dot{V}O_2$ peak) was measured, using an incremental exercise test to volitional exhaustion on a cycle ergometer (Lode, Groningen, The Netherlands). Respiratory gases were measured using an online gas collection system (CORTEX Biophysik MetaLyzer 3B stationary CPX). The test consisted of an initial load of 100 W for 10 min, followed by 30 W increases in external load at 2-min intervals until cadence reduced to < 50 rpm, at which point the test was terminated. $\dot{V}O_2$ peak was reported as the mean oxygen uptake during the final 1-min of exercise.

Stable isotope labelling in vivo

Participants were instructed to maintain their habitual exercise and dietary routine throughout the 12-day D_2O labelling period. Participants recorded the duration and rate of perceived exertion (RPE) of each training session using TrainingPeaks software (TrainingPeaks, Denver, CO, USA). Dietary intake was monitored by recording meal information using a smartphone application (MyFitnessPal, Under Armour, Baltimore, MD, USA) [33].

Biosynthetic labelling of newly synthesised proteins was achieved by oral consumption of deuterium oxide (D_2O). Consistent with our previous work [4, 24], participants consumed 50 ml of 99.8 atom % of D_2O four times per day for days 1–5 commencing after the first muscle biopsy on day 0. On days 6 − 12, the dosage was lowered to 50 ml two times per day. All 50 ml doses were dispensed in a nutrition laboratory and sealed prior to distribution to the participants. Participants were instructed to consume each dose ~ 4 h apart to negate any potential side effects e.g., nausea.

Saliva samples were collected, upon waking, by each participant using pre-labelled saliva collection kits (Salivette, Sarstedt, NC, USA). Participants delivered saliva samples to the laboratory at each visit using a cooled container. Collection tubes were centrifuged for 2 min at 1000 ×*g* and aliquots of saliva were stored at − 80 °C until analysis.

Venous blood samples were collected in EDTA-coated vacutainer tubes via a single use butterfly needle (Beckton Dickson, UK) inserted into the antecubital fossa. Plasma was extracted by centrifugation (1,200 ×*g*, 4 °C for 10 min) prior to storage at − 80 °C for subsequent analysis.

Muscle biopsy protocol

Muscle samples were obtained from the vastus lateralis of the participant's dominant leg after an overnight fast using a Bard Monopty Disposable Core Biopsy Instrument 12-gauge × 10 cm length (Bard Biopsy System, Tempe, AZ). Local anaesthesia (0.5% Marcaine) was administered, and a 0.5 cm longitudinal incision was made through the skin. The muscle fascia was then pierced, and 2–3 muscle pieces were taken to collect adequate amounts (minimum 50 mg) of sample. Samples were blotted to remove excess blood, and visible fat and connective tissue were removed through dissection. Muscle tissue was snap-frozen in liquid nitrogen and stored at − 80 °C for subsequent analysis.

Calculation of D2O Enrichment

Body water enrichment of D_2O was measured in plasma and saliva samples against external standards that were constructed by adding D_2O to PBS over the range from 0.0 to 5.0% in 0.5% increments. Deuterium enrichment of aqueous solutions was determined by gas chromatography–mass spectrometry after exchange to acetone [34]. Samples were centrifuged at 12,000 g, 4 °C for 10 min, and 20 µl of sample supernatant or standard was reacted overnight at room temperature with 2 µl of 10 M NaOH and 4 µl of 5% (v/v) acetone in acetonitrile. Acetone was then extracted into 500 µl chloroform and water was captured in 0.5 g Na_2SO_4 before transferring a 200-µl aliquot of chloroform to an auto-sampler vial. Samples and standards were analysed in triplicate by using an Agilent 5973 N mass selective detector coupled to an Agilent 6890 gas chromatography system (Agilent Technologies, Santa Clara, CA, USA). A CD624-GC column (30 m, 30.25 mm^3 1.40 mm) was used in all analyses. Samples (1 µl) were injected by using an Agilent 7683 autosampler. The temperature program began at 50 °C and increased by 30 °C/min to 150 °C and was held for 1 min. The split ratio was 50:1 with a helium flow of 1.5 ml/min. Acetone eluted at ~ 3 min. The mass spectrometer was operated in the electron impact mode (70 eV) and selective ion monitoring of m/z 58 and 59 were performed by using a dwell time of 10 ms/ion.

Muscle processing

Muscle samples were pulverized in liquid nitrogen, then homogenized on ice in 10 volumes of 1% Triton X- 100, 50 mM Tris, pH 7.4 (including complete protease inhibitor; Roche Diagnostics, Lewes, United Kingdom) using a PolyTron homogenizer. Homogenates were incubated on ice for 15 min, then centrifuged at 1000 ×*g*, 4 °C, for 5 min to fractionate insoluble (myofibrillar) proteins from soluble proteins. Soluble proteins were decanted and cleared by further centrifugation (12,000 ×*g*, 4 °C, for 45 min). Insoluble proteins were resuspended in a half-volume of homogenization buffer followed by centrifugation at 1000 ×*g*, 4 °C, for 5 min. The washed pellet was

then solubilized in lysis buffer (7 M urea, 2 M thiourea, 4% CHAPS, 30 mM Tris, pH 8.5) and cleared by centrifugation at 12,000 ×*g*, 4 °C, for 45 min. Protein concentrations of the insoluble and soluble protein fractions were measured by Bradford assay. Aliquots containing 500 µg protein were precipitated in 5 volumes of ice-cold acetone and incubated for 1 h at − 20 °C. Proteins were then resuspended in lysis buffer to a final concentration of 5 µg/µl.

Tryptic digestion was performed using the filter-aided sample preparation (FASP) method [35]. Aliquots containing 100 µg protein were precipitated in acetone and resuspended in 40 µl UA buffer (8 M urea, 100 mM Tris, pH 8.5). Samples were transferred to filter tubes and washed with 200 µl of UA buffer. Proteins were incubated at 37 °C for 15 min in UA buffer containing 100 mM dithiothreitol followed by incubation (20 min at 4 °C) protected from light in UA buffer containing 50 mM iodoacetamide. UA buffer was exchanged with 50 mM ammonium bicarbonate and sequencing-grade trypsin (Promega, Madison, WI, USA) was added at an enzyme to protein ratio of 1:50. Digestion was allowed to proceed at 37 °C overnight then peptides were collected in 100 µl 50 mM ammonium bicarbonate containing 0.2% trifluoroacetic acid. Samples containing 4 µg of peptides were de-salted using C_{18} Zip-tips (Millipore) and resuspended in 20 µl of 2.5% (v/v) ACN, 0.1% (v/v) formic acid (FA) containing 10 fmol/µl yeast alcohol dehydrogenase (ADH1; MassPrep, Waters Corp., Milford, MA).

Liquid chromatography-mass spectrometry of the myofibrillar protein fraction

Liquid chromatography-mass spectrometry of myofibrillar proteins was performed using nanoscale reverse-phase ultra-performance liquid chromatography (NanoAcquity; Waters Corp., Milford, MA) and online electrospray ionization quadrupole-time-of-flight mass spectrometry (Q-TOF Premier; Waters Corp.). Samples (5 µl corresponding to 1 µg tryptic peptides) were loaded by partial-loop injection on to a 180 µm ID ×20 mm long 100 Å, 5 µm BEH C_{18} Symmetry trap column (Waters Corp.) at a flow rate of 5 µl/min for 3 min in 2.5% (v/v) ACN, 0.1% (v/v) FA. Separation was conducted at 35 °C via a 75 µm ID ×250 mm long 130 Å, 1.7 µm BEH C_{18} analytical reverse-phase column (Waters Corp.). Peptides were eluted using a non-linear gradient that rose to 37.5% acetonitrile 0.1% (v/v) FA over 90 min at a flow rate of 300 nl/min. Eluted peptides were sprayed directly into the mass spectrometer via a NanoLock Spray source and Picotip emitter (New Objective, Woburn, MA). Additionally, a LockMass reference (100 fmol/µl Glu- 1-fibrinopeptide B) was delivered to the NanoLock Spray source of the mass spectrometer at a flow rate of 1.5 µl/min and was sampled at 240 s intervals. For all measurements, the mass spectrometer was operated in positive electrospray ionization mode at a resolution of 10,000 full width at half maximum (FWHM). Before analysis, the time-of-flight analyser was calibrated using fragment ions of [Glu-1]-fibrinopeptide B from m/z 50 to 1990.

Mass spectra for liquid chromatography-mass spectrometry profiling were recorded between 350 and 1600 m/z using mass spectrometry survey scans of 0.45-s duration with an interscan delay of 0.05 s. In addition, equivalent data-dependent tandem mass spectra (MS/MS) were collected from each baseline (day 0) sample. MS/MS spectra of collision-induced dissociation fragment ions were recorded from the 5 most abundant precursor ions of charge 2+ 3+ or 4+ detected in each survey scan. Precursor fragmentation was achieved by collision-induced dissociation at an elevated (20–40 eV) collision energy over a duration of 0.25 s per parent ion with an interscan delay of 0.05 s over 50–2000 m/z. Acquisition was switched from MS to MS/MS mode when the base peak intensity exceeded a threshold of 30 counts/s and returned to the MS mode when the total ion chromatogram (TIC) in the MS/MS channel exceeded 50,000 counts/s or when 1.0 s (5 scans) were acquired. To avoid repeated selection of peptides for MS/MS, the program used a 30-s dynamic exclusion window.

Liquid chromatography-mass spectrometry of the solule protein fraction

Data-dependent label-free analysis of soluble protein fractions was performed using an Ultimate 3000 RSLC nanosystem (Thermo Scientific, Waltham, MA) coupled to a Fusion mass spectrometer (Thermo Scientific). Samples (3 µl corresponding to 600 ng of protein) were loaded on to the trapping column (Thermo Scientific, PepMap100, C_{18}, 75 µm X 20 mm), using partial loop injection, for 7 min at a flow rate of 9 µl/min with 0.1% (v/v) trifluoroacetic acid. Samples were resolved on a 500 mm analytical column (Easy-Spray C_{18} 75 µm, 2 µm column) using a gradient of 96.2% A (0.1% formic acid) 3.8% B (79.9% ACN, 20% water, 0.1% formic acid) to 50% B over 90 min at a flow rate of 300 nL/min. The data-dependent program used for data acquisition consisted of a 120,000-resolution full-scan MS scan (AGC set to 4^{e5} ions with a maximum fill time of 50 ms) and MS/MS using quadrupole ion selection with a 1.6 m/z window, HCD fragmentation and normalised collision energy of 32 and LTQ analysis using the rapid scan setting and a maximum fill time of 35 ms. The machine was set to perform as many MS/MS scans as to maintain a cycle time

of 0.6 s. To avoid repeated selection of peptides for MS/MS the program used a 60 s dynamic exclusion window.

Label-free quantitation of protein abundances

Progenesis Quantitative Informatics for proteomics (Non-Linear Dynamics, Newcastle, UK) was used to perform label-free quantitation on samples collected at days 8 and 12 only. QToF data were LockMass corrected using the doubly charged monoisotopic ion (*m/z* 785.8426) of the Glu- 1- fibrinopeptide B. Prominent ion features were used as vectors to warp each data set to a common reference chromatogram, which avoids misalignment and missing values that can corrupt mass isotopomer analyses [36]. An analysis window of 15–105 min and 350–1500 m/z was selected and Log-transformed MS data were normalized by inter-sample abundance ratio, and relative protein abundances were calculated using unique peptides only. Abundance data were normalised to the median abundance of 3 most abundant peptides of yeast ADH1 [31] to derive abundance measurements in fmol/µg units. MS/MS spectra were exported in Mascot generic format and searched against the Swiss-Prot database (2018.7) restricted to Homo-sapiens (20,272 sequences) using a locally implemented Mascot server (v.2.2.03; https://www.matrixscience.com). Enzyme specificity was trypsin, allowing 1 missed cleavage, carbamidomethyl modification of cysteine (fixed). QToF data was searched using m/z errors of 0.3 Da, whereas FUSION data were searched using MS errors of 10 ppm and MS/MS errors of 0.6 Da. Mascot output files (xml format), restricted to nonhomologous protein identifications, were recombined with MS profile data in Progenesis.

Measurement of protein turnover rates

Mass isotopomer abundance data from samples collected at days 8 and 12 were extracted from MS spectra using Progenesis Quantitative Informatics (Non-Linear Dynamics, Newcastle, UK). Consistent with our previous work, e.g. [30], the abundances of the monoisotopic peak (m_0), m_1, m_2 and m_3 mass isotopomers were collected over the entire chromatographic peak for each proteotypic peptide that was used for label-free quantitation of protein abundances. Mass isotopomer information was processed in R version 3.5.2 (R core team., 2016). Deuterium incorporation into muscle proteins in vivo was calculated from changes in the molar fraction (fm_0) of each peptide monoisotopic (m_0) peak.

$$fm_0 = \frac{m_0}{m_0 + m_1 + m_2 + m_3} \tag{1}$$

Incorporation of D_2O into newly synthesized protein results in a decrease in the molar fraction of the monoisotopic (fm_0) peak that follows the pattern of an exponential decay. The rate constant (k) of the decay in fm_0 was calculated as a first-order exponential spanning from between day 8 (t_0) and day 12 (t) of the experimental period.

$$k = \frac{1}{t - t0} \cdot \mathrm{In}\left(\frac{fm_{0_t}}{fm_{0_{t0}}}\right) \tag{2}$$

The degradation (k_{deg}) rate of each peptide was calculated on a per participant basis by dividing k by the molar percent enrichment of deuterium in the precursor (p) pool of each participant and the total number (n) of ^{2}H exchangeable H—C bonds in each peptide, which was referenced from standard tables [37]

$$k_{deg} = \frac{k}{(n \bullet p)} \tag{3}$$

Fractional turnover rate (FTR; %/d) was calculated from the median K_{deg} of peptides assigned to each protein in each participant and decimal K_{deg} data were multiplied by 100 to give fractional turnover rates in %/d units.

$$FTR = k_{deg} \cdot 100 \tag{4}$$

Protein half-life (d) was calculated by dividing the natural log of 2 by K_{deg}.

$$t_{1/2} = \frac{\ln(2)}{k_{deg}} \tag{5}$$

Mole turnover rate (MTR; fmol/µg protein/d) of each protein was calculated by multiplying participant specific k_{deg} by the average abundance of the corresponding protein abundance (ABD; fmol/µg protein) measured in each individual at the beginning (t_0) and end (t) of the labelling period.

$$MTR = k_{deg} \cdot \left(\frac{ABD_{to+}ABD_t}{2}\right) \tag{6}$$

Absolute turnover rate (ATR; ng/µg protein/d) of each protein was calculated by multiplying participant-specific MTR data by the molecular weight (MW; Da) of each protein predicted in the UniProt Knowledgebase.

$$ATR = MTR \cdot \mathrm{MW} \tag{7}$$

Bioinformatic analysis

Functional annotation and the association of proteins with pathways of the Kyoto Encyclopaedia of Genes and Genomes [KEGG; https://www.genome.jp/kegg/, [38]] were conducted using the Perseus platform [39]. Protein interactions were investigated using bibliometric mining in the Search Tool for the Retrieval of Interacting Genes/

proteins (STRING; https://string-db.org/) [40]. Protein physio-chemical characteristics, including isoelectric point (*pI*) and molecular weight (MW) were calculated using the Swiss Institute of Bioinformatics EXpasy ProtParam tool (https://web.expasy.org/protparam/). Statistical analysis was performed in R (Version 3.6.2). Within-subject differences between samples collected on day 8 and day 12 were investigated by repeated measures one-way ANOVA. Significance was identified as $P \leq 0.05$ and a false-discovery rate of 5% calculated from q-values [41]. Differences amongst myosin heavy chain (MyHC) isoforms and the subunits of multiprotein complexes were investigated by one-way ANOVA with Tukey's HSD post-hoc analysis. Pearson's moment correlation analyses were used to determine relationships between protein abundance and turnover rate expressed in relative (e.g., FTR or $t_{1/2}$), mole and absolute units. Amino acid sequence logos were generated using Seq2Logo 2.0 (https://services.healthtech.dtu.dk/services/Seq2Logo-2.0/). Stoichiometry of multiprotein complexes were calculated and compared to the expected stoichiometry reported within The Complex Portal [42]. Gene ontology analysis was conducted on the top quantile of proteins when ranked by ABD, FTR, MTR and ATR using cluster profiler with significance set at an adjusted *P* value ≤ 0.05.

Results

Protein abundance measurements

Three physically active age-matched males were studied that had similar peak aerobic capacity and body mass index (Table 1). In total, 1,885 proteins were identified and 1,772 of these proteins had at least 1 unique peptide (< 1% FDR) detected in both day 8 and day 12 samples in all 3 participants. The abundance of muscle proteins spanned 6 orders (Fig. 2A) of magnitude from 0.003 fmol/µg (leucine tRNA Ligase; SYLC) to 4146.35 fmol/µg (haemoglobin subunit beta; HBB). There were no statistically significant differences in protein abundance between day 8 and day 12 and the R^2 for protein abundance data was 0.987 (Fig. 2B). The median coefficient of variation in protein abundance was 6% with an interquartile range from 2.97% to 12.54%, which demonstrates a high level of repeatability between protein abundance measurements at day 8 and day 12. Therefore, we did not include adjustments for differences in protein abundance in our calculation (Eq. 2) of the rate constant (*k*) for the incorporation of deuterium into proteins. Gene ontology analysis of the upper quartile (n = 234 proteins) of protein abundances, included proteins associated with muscle contraction, muscle system process, regulation of muscle contraction, sarcomere organization and striated muscle contraction as the most enriched processes in human muscle (Fig. 2C). Whereas biological processes, including tRNA aminoacylation, positive regulation of transcription, protein folding, cell migration and regulation of translation were enriched amongst proteins in the lower quartile of abundance measurements.

Table 1 Participant characteristics

	X	Y	Z
Age (y)	21	22	22
Height (m)	1.79	1.77	1.78
Weight (kg)	72.20	69.10	79.70
BMI (kg/m^2)	23.50	21.10	25.30
$\dot{V}O_2$ peak (L/min)	3.59	3.79	4.27
$\dot{V}O_2$ peak (ml/kg/min)	49.9	54.8	53.6
Peak Power Output (W)	280	280	340

Protein turnover measurements

Body water enrichment measured in blood plasma rose at a rate of 0.3 ± 0.032%/d during the first 6 days of deuterium oxide consumption then plateaued and was not different ($P = 0.1058$) between day 8 (1.71 ± 0.08%) and day 12 (1.89 ± 0.07%). Stringent filters were applied to select peptides with clearly resolved envelopes of m_0, m_1, m_2 and m_3 mass isotopomers, and in all 6,800 protein-specific peptides met the inclusion criteria for turnover calculations in one or more participants. The turnover rates of 935 proteins were measured in at least 1 participant (Suppl Table S1), whereas data were collected for 766 proteins in 2 or more participants and the turnover rate of 444 proteins was measured in all 3 participants. Unless otherwise stated, data are presented from at least n = 2 participants in the subsequent text and figures. The turnover of individual proteins in human vastus lateralis in vivo ranged from 0.32%/d (microtubule associated protein RP/EB family member 2; MARE2) to 54.43%/d (nuclear protein localisation protein 4 homolog; NPL4) and the median (IQR) of protein-specific FTR was 4.3 (2.52–7.84) %/d. MTR had a median of 0.04 (IQR: 0.01–0.10) fmol/µg/d and ranged between 0.00013 (MARE2) and 56.89 fmol/µg/d haemoglobin subunit beta (HBB). ATR values had a median of 1.53 (IQR: 0.48–4.63) ng/µg/d and ranged between 0.005 (MARE2) and 931.98 ng/µg/d (albumin; ALBU). Different gene ontological classifications were highlighted amongst the 75th percentile of proteins when turnover data were presented in relative or absolute units (Fig. 2). When ranked by FTR, cellular oxidant detoxification, cellular response to toxic substance, nuclear migration, nucleus localization and viral process were amongst the top-ranked terms. (Fig. 2D). In contrast, proteins ranked in the 75th percentile by MTR were associated with terms, multicellular organismal

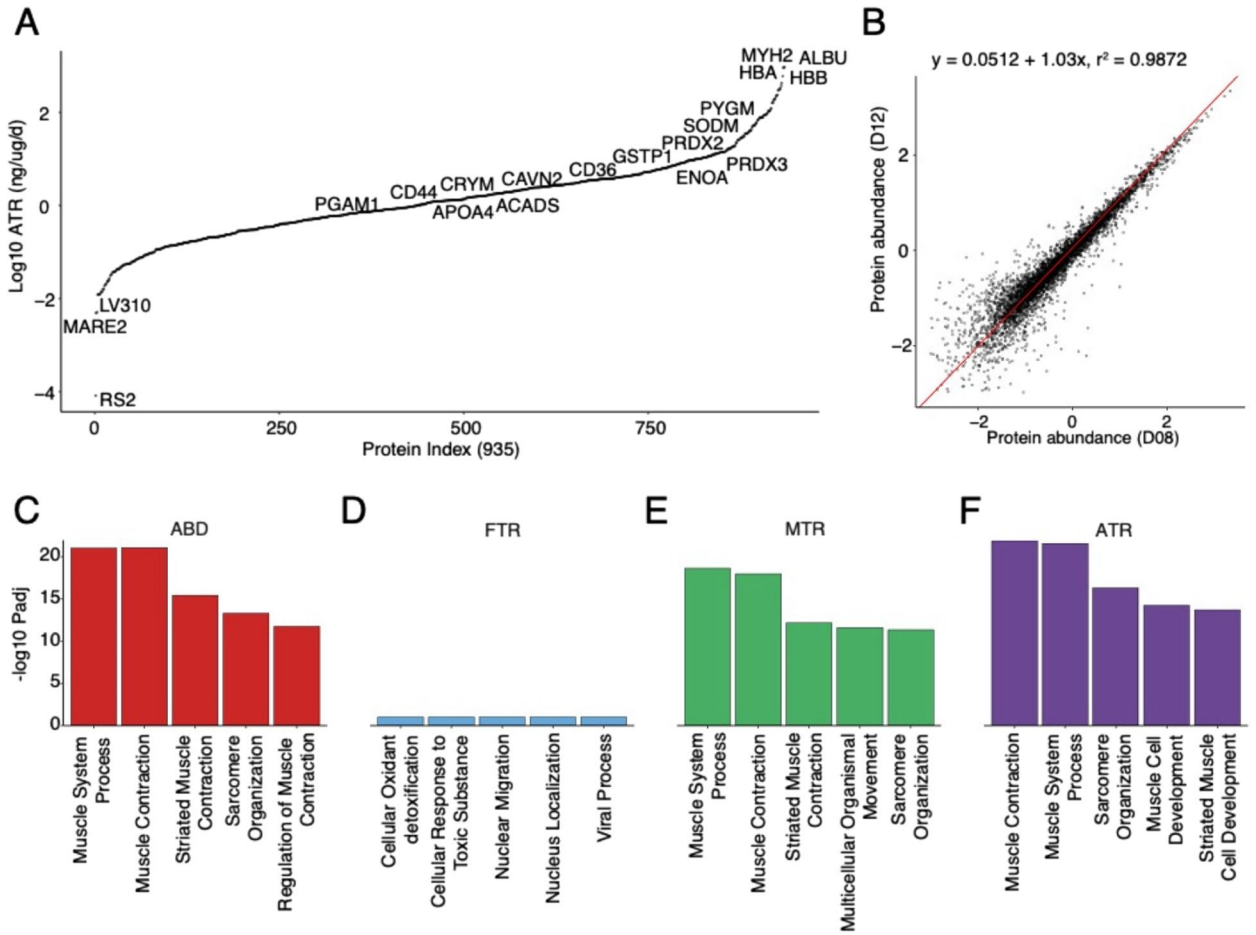

Fig. 2 Proteome profiling of human vastus lateralis muscle in vivo.Proteins were extracted from the vastus lateralis of humans and turnover rates for 935 proteins were quantified in at least one participant. **A** Log10 transformed distribution plot, of proteins ranked by ATR (ng/μg/d). Proteins of interest are labelled using their UniProt ID. **B** Linear regression of within-subject protein abundance data at day 8 and day 12. Panels C-F report the 5 most significant enriched GO Biological Processes amongst the top-ranking proteins contained within the upper quartile when the protein dataset was ranked by either (**C**) abundance, (**D**) fractional, (**E**) molar or (**F**) absolute turnover rate

movement, muscle contraction, muscle system process, sarcomere organization, and striated muscle contraction (Fig. 2E). And proteins ranked in the 75th percentile by ATR were associated with the terms muscle cell development, muscle contraction, muscle system process, sarcomere organization and striated muscle cell development (Fig. 2F). Furthermore, antioxidant enzymes, including SODM (mitochondrial superoxide dismutase [Mn]), PRDX3 (peroxiredoxin 3), PRDX2 (peroxiredoxin 2) and (GSTP1) glutathione S-transferase-P were also amongst the top-ranked proteins by ATR, consistent with their prominent role in skeletal muscle physiology.

Our analysis encompassed 35 myofibrillar proteins, including each of the main components of the sarcomere (Fig. 3), which were primarily extracted from the insoluble fraction. The myosin heavy chain (MyHC) isoform profile was 65 ± 2.4% type IIa (MYH2), 24 ± 3.5% type I (MYH7) and 12 ± 1.2% type IIx (MYH1). Accordingly, the abundance (ABD) of MYH2 (634.50 ± 173.79 fmol/μg) was significantly ($p \leq 0.01$) greater than MYH1 (114.67 ± 38.25 fmol/μg) and MYH7 (225.97 ± 24.96 fmol/μg), whereas there were no significant differences amongst turnover of MyHC isoforms (Fig. 3B) when expressed in FTR (%/d) units. When rate data were expressed in mole (Fig. 3C) or absolute terms (Fig. 3D), the turnover profile of MyHC isoforms more closely mirrored the abundance data and both the MTR (8.07 ± 1.93 fmol/μg/d) and ATR (1799.2 ± 429.82 ng/μg/d) of MYH2 were significantly ($p \leq 0.01$) greater than MYH7 (MTR; 2.56 ± 1.13 fmol/μg/d, ATR; 571 ± 252.3 ng/μg/d) and MYH1 (MTR; 2.03 ± 1.04 fmol/μg/d, ATR; 453.70 ± 232.19 ng/μg/d).

Protein turnover data were collected for 48 proteins of the major energy metabolism pathways in human muscle (Fig. 4), including fatty acid β-oxidation (17 of 42 annotated in gene ontology databases), glycolysis (15 of 67) and the TCA cycle (16 of 30). The median

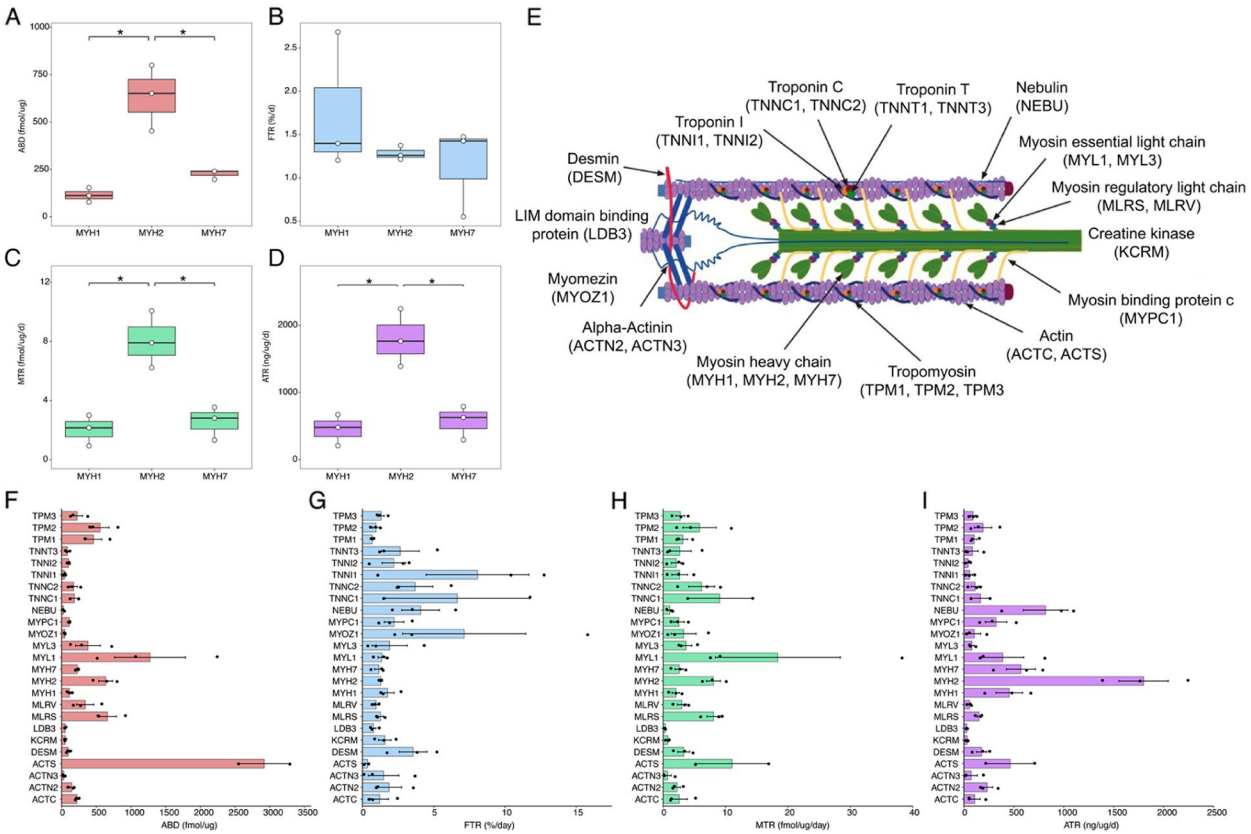

Fig. 3 Turnover rates of muscle sarcomeric proteins. Individual data points with box plot-style overlay representing the MyHC profile of the vastus lateralis are displayed for abundance (**A**), FTR (**B**), MTR (**C**) and ATR (**D**) measurements ($N = 3$). *Significant ($P \leq 0.05$) differences between proteins determined by ANOVA and TUKEY's HSD. Panel E is a visual representation of the skeletal muscle sarcomere with major proteins labelled. Protein abundance (**F**), FTR (**G**), MTR (**H**) and ATR (**I**) measurements for sarcomeric proteins detected in the insoluble fraction ($N = 2$–3; presented as individual points and bars represent mean values ± SE). All proteins are labelled using their UniProt ID

(IQR) ABD of proteins involved in fatty acid oxidation and the TCA cycle were 2.11 (IQR; 1.13–3.65) fmol/μg and 3.34 (IQR; 0.63–8.41) fmol/μg respectively, whereas the ABD for proteins involved in glycolysis was approximately tenfold greater, 37.00 (IQR; 9.12–105.56) fmol/μg. Despite the markedly greater abundance of glycolytic enzymes, the median FTR (2.10, 1.20–2.40%/d) of glycolytic proteins was not different from enzymes of either TCA cycle (2.20, 1.66–3.04%/d) or fatty acid oxidation pathway (2.78, 2.19–3.94%/d). Differences amongst the turnover of proteins of the different metabolic pathways were more transparent when data were expressed in mole or absolute units. The MTR (0.69, 0.15–1.34 fmol/μg/d) and ATR (29.23, 7.84–81.48 ng/μg/d) of enzymes involved in glycolytic processes was ≥ tenfold greater than the TCA cycle (MTR; 0.077, 0.022–0.134 fmol/μg/d, ATR; 4.06, 1.24–9.41 ng/μg/d) and fatty acid oxidation (MTR; 0.065, 0.039–0.095 fmol/μg/d, ATR; 2.12, 1.29–3.63 ng/μg/d).

Predictors of protein turnover rates in human muscle in vivo

Protein turnover expressed in fractional units (FTR, %/d) did not correlate ($r = -0.082$) with mole protein abundance (Fig. 5A), whereas ABD and MTR share the same units (i.e. fmol/μg) and exhibited a strong ($r = 0.9695$) positive relationship (Fig. 5B). The positive correlation lessens ($r = 0.6964$) (Fig. 5C) between ABD and ATR because high MW proteins are not necessarily the most abundant in skeletal muscle. Neither protein molecular weight (MW; Fig. 5 D-F) nor isoelectric point (p*I*; Fig. 5 G-I) corelated with protein turnover expressed in either relative or absolute units. The median (IQR) for p*I* and MW of proteins in the current study were 41.44 (IQR;

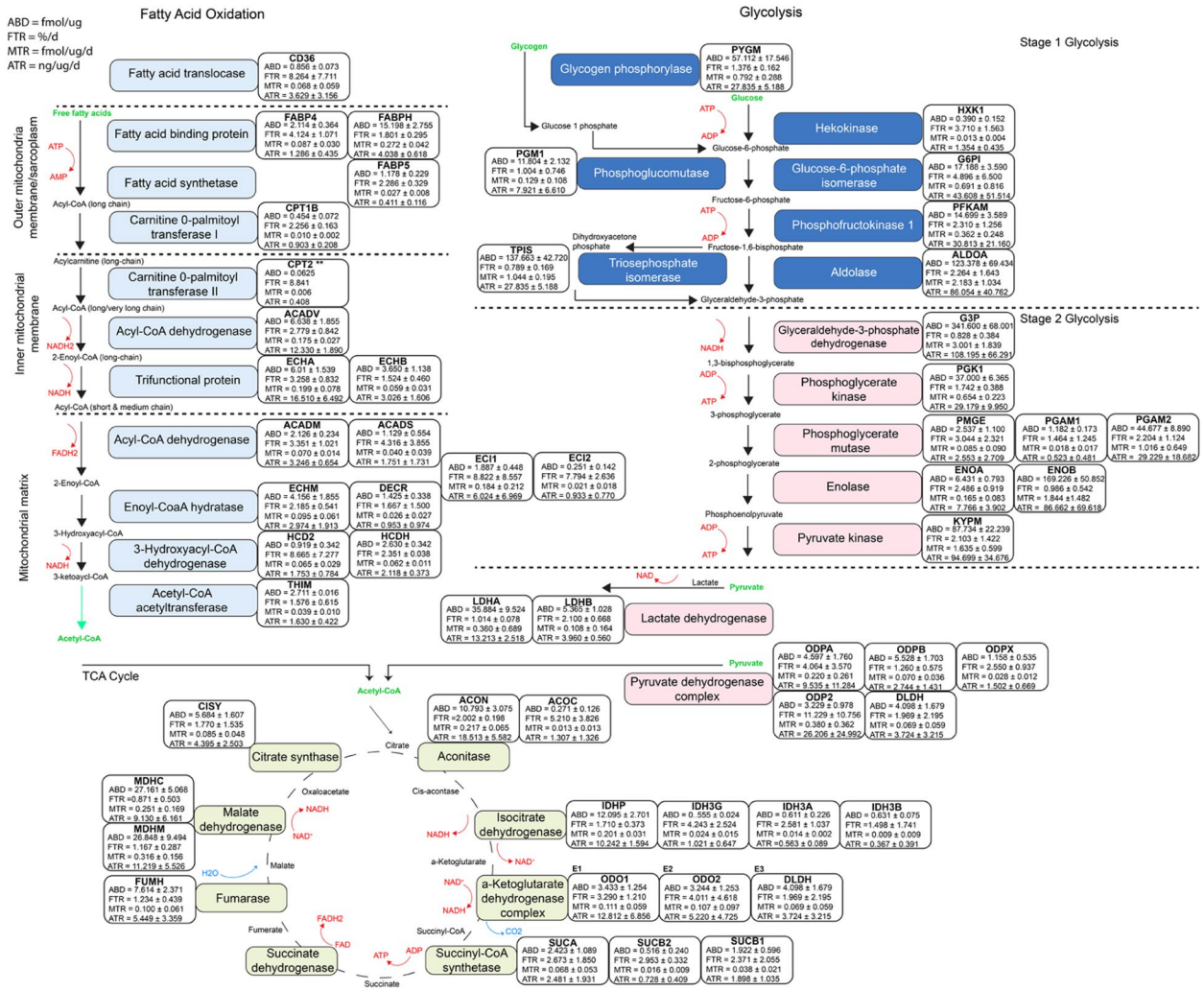

Fig. 4 Proteomic profiling of metabolic enzyme pathways. Individual protein abundance (ABD) turnover rates in fractional (FTR), mole (MTR) and absolute (ATR) units for proteins involved in fatty acid oxidation, glycolysis and the TCA cycle are reported. Data are mean ± SD from $n =$ 2–3 participants except for CPT2, which was measure in 1 participant only. Common names of proteins are labelled in coloured boxes, with adjacent boxes labelled using UniProt protein IDs

25.97–63.45) KDa and pH 6.105 (IQR; 5.37–7.58). Pearson's corelation analysis of the top 50 proteins with the lowest and highest $t_{1/2}$ values found no correlation ($r = -0.0024$) with predicted protein $t_{1/2}$ values calculated using the N-end rule of degradation. Similarly, there was no significant enrichment of linear motifs amongst either the top (Fig. 5K) or bottom-ranked proteins (Fig. 5L).

Subunit stoichiometry of multiprotein complexes

Data were collected for 79 subunits of 6 multiprotein complexes (MPC), including the 26S proteasome and complexes I, II, III, IV and V of the mitochondrial respiratory chain (Fig. 6). On average the mean ± SD mole abundance of the 26S proteasome (0.342 ± 0.224 fmol/µg) was significantly less ($P \leq 0.05$) than the abundance of respiratory chain complexes III, IV and V (Fig. 6A). Subunits of Complex I (1.414 ± 0.856 fmol/ug) were significantly less abundant than subunits of Complex III (7.311 ± 4.453 fmol/µg) and Complex V (11.335 ± 14.349 fmol/ug). Similarly, subunits of Complex II (2.328 ± 1.944 fmol/ug) and complex IV (4.833 ± 3.835 fmol/ug) were also significantly less abundant than Complex V. There were significant ($P \leq 0.05$) differences in FTR (%/d) between the 26S proteasome and mitochondrial respiratory chain complexes III and V (Fig. 6B). In contrast to ABD data the turnover of the 26S proteasome subunit (8.436 ± 7.03450%/day) was significantly higher than that of Complex III (1.946045 ± 0.479%/day) and Complex V

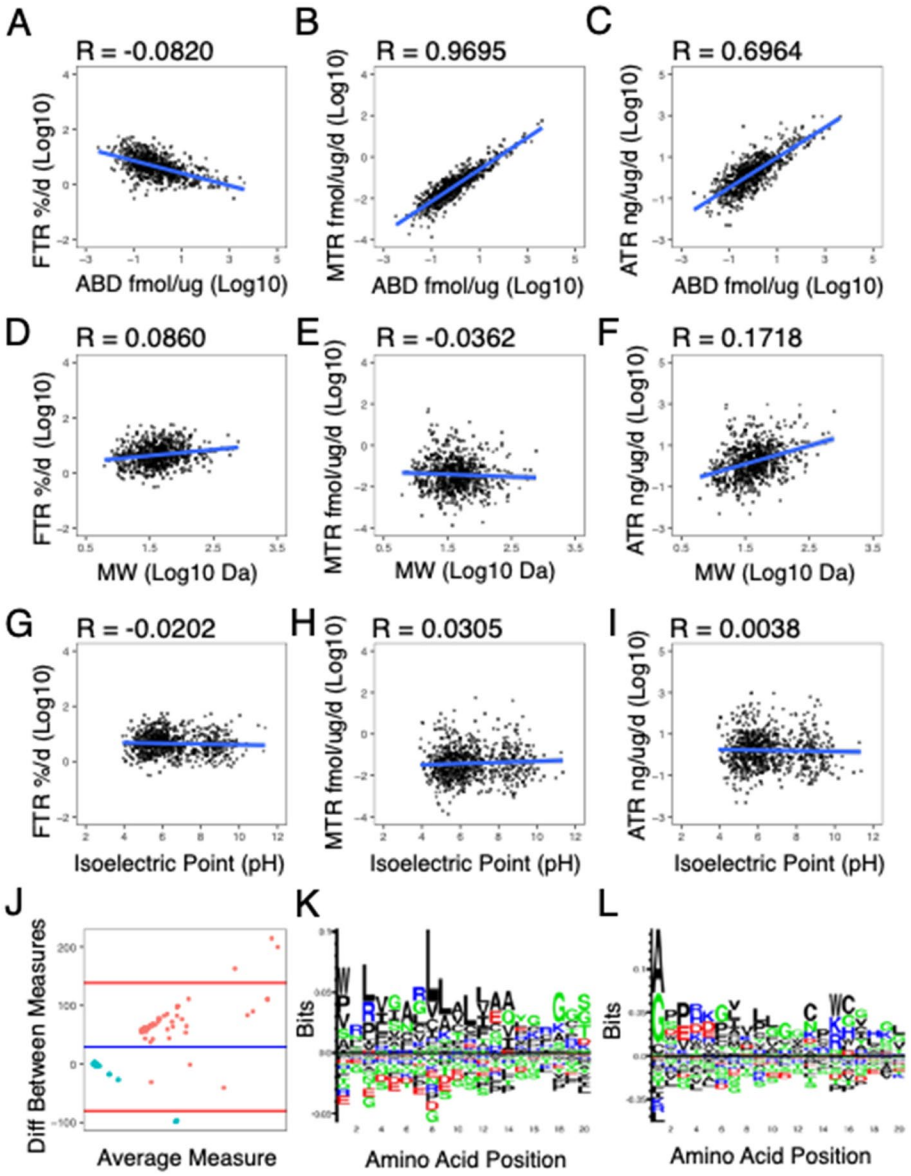

Fig. 5 Predictors of Protein Turnover Rates. (**A-I**) Each turnover measurement was correlated (Pearson's) with protein abundance, MW, and P/ to attempt to predict the turnover of individual proteins. (**J**) Bland Altman plot of the top 50 proteins with the shortest (blue) and longest (red) protein $t_{1/2}$ values against the predicted protein $t_{1/2}$ values calculated using the N end rule of degradation. (**K-L**) P weighted Kullback–Leibler logos of the top quartile (**K**) and bottom (**L**) quartile of proteins ranked by $t_{1/2}$

(2.210 ± 1.091%/day). Turnover data expressed in mole (Fig. 6C) and absolute terms (Fig. 6D) were in better agreement with protein abundance measures, for example Complex IV (0.21 ± 0.25 fmol/μg/day) and Complex V (0.180 ± 0.181 fmol/ug/day) had significantly ($P \leq 0.05$) greater mean ± SD MTR than the 26S proteasome (0.027 ± 0.029 fmol/μg/day). Complex IV also had a significantly higher MTR than complex I (0.09 ± 0.12 fmol/μg/day). Absolute values of MPC highlighted the ATR of Complex V was significantly ($P \leq 0.05$) greater (6.83 ± 11.62 ng/μg/day) than complex I (2.46 ± 3.66 ng/μg/day) and the 26S proteasome (1.02 ± 0.98 ng/μg/day).

Individual subunits within a MPC display differing turnover rates. We identified 18 of the 47 subunits of the 26S proteasome in at least $n = 2$ participants and 24 subunits in $n = 1$ participants (Fig. 7). Ten subunits belonged to the 20S core particle and 13 to the 19S regulatory particle. FTR values of subunits within the 26S proteasome ranged from 1.57 ± 1.06%/d (proteasome subunit alpha type 3; PSA3) to 27. 09 ± 17.50%/d (26S

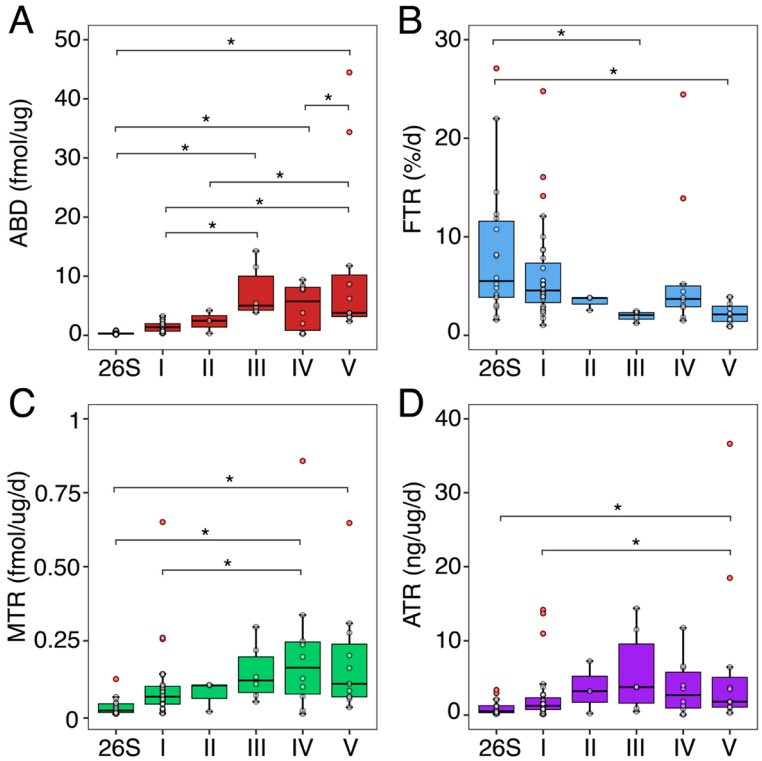

Fig. 6 Proteomic profiling of multiprotein complexes in humans in vivo. Representative box plots of the ABD (**A**), FTR (**B**), MTR (**C**) and ATR (**D**) for proteins identified within each of the mitochondrial respiratory chain complexes (I-V) and the 26S proteasome. Individual dots represent mean values ($n = 2$–3 participants) for each protein within each multiprotein complex (MPC). Outliers are highlighted in red and median values for the corresponding MPC are indicated by solid black lines within the box plot. * Indicate complexes that are significantly different from one another as determined by ANOVA and Tukey's HSD ($P \leq 0.05$)

proteasome AAA-ATPase subunit RPT1; PRS7), with a combined median of 5.50%/d (IQR; 3.86–11.58) for the 18 proteins identified in the current work. MTR and ATR values ranged from 0.003 ± 0.002 fmol/μg/d (PSA3) to 0.12 ± 0.16 fmol/μg/d (proteasome subunit alpha type 7; PSA7) and 0.09 ± 0.06 ng/μg/d (PSA3) to 3.38 ± 4.59 ng/μg/d (PSA7) respectively. The median (IQR) MTR and ATR for the 18 proteins identified in the 26S proteasome are reported as 0.015 (0.008–0.038) fmol/μg/d and 0.51 (0.31–1.27) ng/μg/d respectively.

Complex V of the mitochondrial respiratory chain is a well-defined MPC. We herein quantified the ABD and stoichiometry of Complex V (ATP synthase) and compared the measured protein abundance of each subunit, against their predicted abundance from the Complex Portal database (Fig. 8A). We also compared individual protein subunit turnover in fractional (Fig. 8C), mole (Fig. 8D) and absolute (Fig. 8E) terms against protein abundance stoichiometry. Figure 8F-H illustrates the relationship between the turnover rates and relative protein abundance of subunits of ATP synthase. Values are expressed as a percentage of the total of ATP synthase. There was no relationship ($r^2 = -0.144$) between the FTR of a subunit and its relative protein ABD within the ATP synthase MPC (Fig. 8F). For example, ATPB made up ~37% of the ABD of ATP synthase, but only 6% of turnover (FTR). In contrast, MTR ($r^2 = 0.851$) and ATR ($r^2 = 0.933$) data exhibited significant relationships with the relative ABD of ATP synthase subunits (Fig. 8 G-H). The measured stoichiometry of the average abundance of ATP synthase subunits when normalised to ATPG (i.e. abundance ATPA:ATPB:ATPD per fmol of ATPG) was 9.17: 11.62: 0.84 fmol/μg per fmol/μg of ATPG.

Discussion

Currently few data exist on protein-specific turnover in human skeletal muscle in vivo, and the turnover rates of individual proteins have seldom been reported alongside protein abundance measurements or considering differences in molecular weight amongst proteins. Muscle is renowned for its plasticity and can exhibit a broad range of different phenotypes underpinned by different protein abundance profiles. Therefore, it may be important to consider the abundance of muscle proteins alongside protein-specific turnover data. Herein, we report that the unit of measurement used for dynamic proteomic

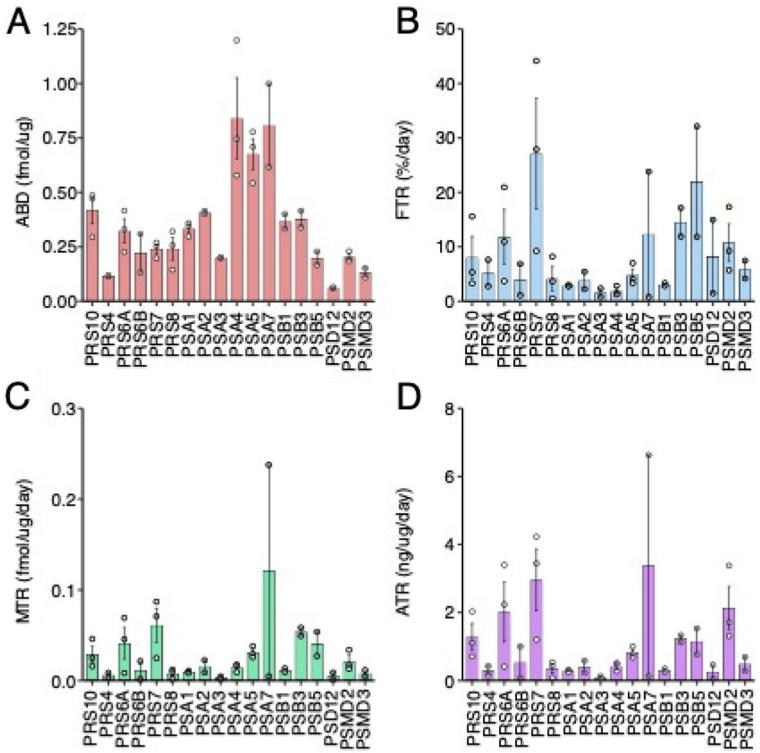

Fig. 7 Proteomic profiling of individual subunits of the 26S Proteasome. Proteomic data were extracted for individual proteins contained within the 26S proteasome ($n = 2–3$ participants). ABD (**A**), FTR (**B**), MTR (**C**) and ATR (**D**) measurements are reported. Bars and error-bars represent mean ± SD, respectively. Points represent values for individual participants

data influences the biological interpretation of the findings. Although commonplace, the presentation of protein turnover or synthesis data in fractional terms (i.e. %/d), masks the different size (molecular weight; MW) and abundance of individual proteins. Data presented in mole units that account for differences in MW amongst protein subunits may be preferred for studies on multiprotein complexes within samples or subcellular fractions. Alternatively, data in absolute units that account for differences in protein abundance between samples may be preferred for studies on longitudinal adaptation or cross-sectional analyses on differing populations.

Changes in protein abundance are underpinned by the balance between the synthesis and degradation of individual proteins [19] but this relationship does not equate to a correlation between the fractional turnover rate of a protein and its abundance (Fig. 5). Disparities between the FTR and abundance of proteins make it difficult to draw conclusions about the physiological state of muscle from FTR data alone [30, 43]. Gene ontology analysis of FTR data highlighted biological processes (Fig. 2) that are not usually viewed as being prominent in healthy muscle and provide limited insight into the allocation of cellular resources or top-ranking molecular processes. Protein turnover is an energy requiring process and higher molecular weight proteins require the formation of more peptide bonds during translation or cleavage of more peptide bonds during proteasomal degradation than smaller proteins. Mole turnover rates incorporate quantification of protein abundance in mole terms and provide new insight into the allocation of cellular resources as well as stoichiometric relationships amongst the synthesis of subunits that form multiprotein complexes in muscle (Fig. 6). Both mole and absolute synthesis rates incorporate protein abundance and so correlated (Fig. 5) with protein abundance measurements and better reflected the biological processes associated with skeletal muscle (Fig. 2).

The median FTR of 935 proteins in human vastus lateralis muscle was 4.3 (IQR 2.52–7.84) %/d, which equates to a median protein half-life of 16 (IQR 9–27) days. These values appear to differ from values (~ 1–2%/d) reported in previous D2O proteomic studies [23, 24] that surveyed fewer proteins, or data on mixed-protein turnover rates derived from the analysis of amino acid hydrolysates, e.g. [44]. In proteomic studies, as the depth of coverage (i.e. number of proteins studied) increases it becomes increasingly important to account for the abundance and

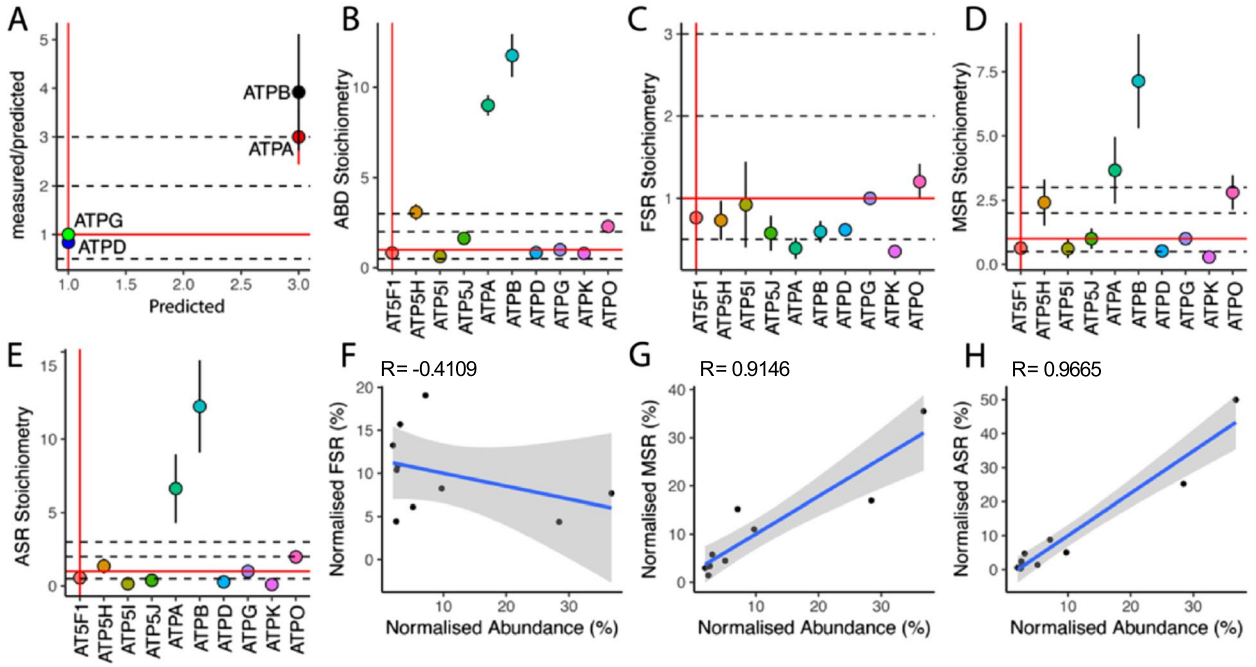

Fig. 8 Subunit stoichiometry of mitochondrial respiratory chain Complex V—ATP Synthase, and relationship between protein turnover and protein abundance. **A** Predicted vs measured abundance values of subunits with known stochiometric ratios in humans normalized to the γ-subunit (ATPG), which forms the central stalk of ATP synthase. The stoichiometry for all quantified subunits in the data set are reported for ABD (**B**), FTR (**C**), MTR (**D**) and ATR (**E**). Protein measurements are normalised to the regulatory subunit ATPG. Measurements of ATPG are represented by red lines and dashed lines represent 0.5 × 2x and 3 × the reported value of ATPG. Correlation between the abundance of subunits of ATP synthase and turnover rates in (**F**) fractional, (**G**) molar and (**H**) absolute units

molecular weight of each protein when estimating the gross average turnover of muscle protein. Large or highly abundant proteins (e.g., myosin and actin) contribute more to the gross average turnover of protein in muscle than less abundant proteins that may exhibit relatively higher rates of turnover. For example, when our FTR data is weighted using absolute abundance values, (i.e. ATR) the pooled FTR for human vastus lateralis muscle was 1.4%/d and in line with previous findings in active individuals. Notably, muscle proteins that exhibit high ATR values and therefore contribute the most to the gross average turnover rate, include blood proteins (e.g. albumin and haemoglobin subunits), myoglobin (MYG) and glycolytic enzymes. In total, the top 10 proteins ranked by ATR account for almost 30% of protein turnover in human skeletal muscle. The prominent contribution of blood proteins and glycolytic enzymes sheds new light on the interpretation of earlier mixed protein FTR data generated by analysis of amino acid hydrolysates. Such analyses of muscle sarcoplasmic fractions often failed to find differences in response to ageing or diet and exercise interventions. If the small number of top-ranking ATR proteins are unaffected by the intervention this will overshadow potentially important responses by proteins that rank lower in ATR but are nonetheless biologically important in muscle.

Because FTR data do not consider the different abundances or molecular weights of the proteins studied, data expressed in MTR or ATR units may be more appropriate for investigating the stoichiometry amongst subunits of multi-protein complexes. Consistent with studies in yeast [45], we report the half-life of 26S proteasome subunits is shorter than that of most respiratory chain subunits. However, the relative abundance of respiratory chain complexes is greater than the proteasome. The mitochondrial respiratory chain comprises five multi-protein complexes and the relative combination and organisation of each complex influences mitochondrial super complex formation [46], and is crucial for subunit-complex stability [47]. The stoichiometry amongst subunits may be adaptable, for example differences in physical activity levels [48] and exercise training [49] are associated with different abundance profiles of respiratory chain protein subunits. ATP-synthase (respiratory chain Complex V) is responsible for ATP resynthesis [50], and defects in ATP-synthase structure are associated with diseases and ageing [51], whereas the beta subunit of ATP-synthase is particularly responsive to exercise [52].

We quantified the ABD of individual proteins constituting the ATP-synthase complex to investigate the stoichiometry amongst its subunits and their turnover rates in human muscle in vivo. Data were normalised to ATPG, which constitutes the singular central stalk (gamma subunit) of each ATP synthase multiprotein complex. A stoichiometry of 1:9:12 was found between ATPG: ATPA and ATPB abundance, which differs from human mitochondrial DNA models in yeast [53] that report ATP-synthase contains 3 subunits each of ATPA and ATPB for every 1 subunit of ATPG. The greater ratio of ATPA and ATPB subunits in human muscle in vivo may indicate a pool of subunits that are not assembled into mature complexes. This could either present a burden to proteostasis mechanisms, including transport systems of the inner and outer mitochondrial membranes, or represent a beneficial, ready source of replacement subunits that helps to maintain the quality of the multiprotein complex. The FTR of ATP synthase subunits was similar when normalised relative to the FTR of ATPG, but the relative relationship between subunits was different (Fig. 8) when data were expressed in MTR units. While our current data can be used for within-sample comparisons of FTR, MTR and ATR data, further work is required to investigate the stoichiometry of ATP-synthase subunits using purified subcomplexes or mitochondria-enriched fractions. Notably, our current data from the soluble protein fractions, which encompasses both cytosolic and mitochondrial compartments cannot distinguish complexes from individual subunits or the potential different cellular locations of proteins.

Theoretically, the turnover rate of a protein may be dictated by both its intrinsic properties, including sequence motifs and physiochemical properties, and by extrinsic factors, including the cell environment and regulatory processes acting on protein translation and degradation. In HeLa cells, highly abundant proteins have slower than average synthesis rates than low abundant proteins [54] and in our data (Fig. 5A) FTR also tended to be inversely related (r- 0.082) to protein abundance. In yeast, the intrinsic properties of proteins, including physiochemical properties, linear sequence motifs, biological function and mRNA half-life, provide some predictive relationship with protein turnover under stable culture conditions [45]. N-terminal linear sequence motifs have been associated with high- and low-turnover rate proteins but we report no relationship between N-terminal sequence and protein half-life (Fig. 5J), which is consistent with earlier studies using sequence information from protein databases [9, 54], or empirically determined sequences of N-terminal peptides using tandem mass spectrometry [55]. We also found the intrinsic properties of a protein such as their predicted molecular weight (MW) and isoelectric point (p*I*) have little to no relationship with protein turnover rates in vivo reported in FTR units (Fig. 5), which is consistent with studies in human cells in vitro [9, 54]. When studied using 2-dimensional gel electrophoresis, the majority of human muscle proteins resolve as multiple proteoforms [56], which cannot be distinguished in LC–MS/MS analyses of tryptic peptide digests used here and in previous studies [9, 54]. In particular, proteoforms with different post-translational modifications may exhibit marked differences in p*I* from their predicted values and this may contribute to the lack of association between FTR and predicted p*I* in the current data. However, in rat soleus [57], proteoforms of creatine kinase share similar turnover rates, whereas the turnover rate differed between the 2 proteoforms of albumin studied.

The half-life of proteins is shorter in vitro compared to studies on intact tissue in vivo [11]. In addition, the influence of extrinsic factors on the turnover of proteins may be more prominent in vivo than in vitro, even when studied, as here, under steadystate conditions. In rats the turnover rate of a particular protein in vivo is not always consistent across different muscles from an individual animal [57]. For example, the FTR of the primary proteoform of the blood protein, albumin, is similar (range 4.8%/d – 6.3%/d) regardless of whether the data is extracted from samples of heart, diaphragm, soleus or extensor digitorum longus. In contrast, the FTR of the cardiac/slow muscle myosin essential light chain (MYL3) is 7.4%/d in EDL, 10.7%/d in diaphragm and 6.4%/d in heart [57]. Moreover, the rank order of protein turnover rates is not consistent amongst different muscles [57] and the turnover rate of a protein can change in response to environmental stimuli, including muscle contraction and exercise training [4, 19]. Therefore, attempts to predict protein turnover in vivo from the intrinsic properties of the protein seem unlikely to be rewarding.

In the current work we have studied human muscle under steadystate conditions of precursor enrichment and protein abundance. Under such constraints, the incorporation of deuterium into protein can be modelled as an exponential decay in fM0 (Eq. 2) that reflects the contributions of both synthesis and degradation to the replacement (i.e. turnover) of the protein pool [12]. At the onset of the labelling period, the probability that a newly synthesised protein will include deuterium label is set by the level of precursor enrichment, whereas protein degradation is likely to remove unlabelled protein, i.e. given that the large existing pool of protein is unlabelled. Therefore, label is incorporated into protein relatively rapidly before reaching a plateau as a balance is neared between the probability that synthesis will add label to the protein pool (i.e.

dictated by precursor enrichment) and degradation will remove label from the protein pool (i.e. assuming degradation is a stochastic process with equal preference for labelled and unlabelled protein) [12]. Our current work illustrates how parallel analysis of the size of the protein pool (i.e. protein abundance) can add context to the interpretation of protein turnover data. In addition, measurement of protein abundance is critical in circumstances where protein abundance may be changing. Equation 8 illustrates how changes in protein abundance (P) between the beginning (t0) and end (t) of the labelling period can be accommodated into Eq. 2.

$$k = \frac{1}{t - t_0} \cdot -\mathrm{In}\left(\frac{fm_0(t)}{fm_0(t_0)}\right) \cdot \frac{P(t)}{P(t_o)} \quad (8)$$

The inclusion of protein abundance (P) data into rate equations is particularly important for studying individual proteins under non-steadystate conditions and does not necessarily need to be in mole or absolute units, for example fold-differences can be used. It should be noted, however, there are assumptions to the calculations of protein dynamics, which may not be met in all experimental systems. The equations assume all proteins have an equal probability of being degraded but both the ubiquitin proteasome and autophagy systems can be a modulated and protein-selective processes, and in circumstances such as ageing, the muscle of older animals may contain insoluble protein aggregates [58] that could affect the calculation of protein turnover rates.

Studies on protein turnover rates must also consider the duration of the labelling period and the time points at which samples are taken. In the current work, participants followed a five-day regimen of deuterium oxide loading, which was designed to steadily raise deuterium enrichment and avoid feelings of nausea and dizziness that can occur when larger boluses of deuterium oxide are consumed [59]. Protein turnover rates were calculated from changes in peptide mass isotopomer profiles between days 8 and 12, which coincided with the period when deuterium enrichment of the precursor pool was unchanging. The relatively short (4-day) investigation period means proteins with low rates of turnover may not exhibit detectable changes in mass isotopomer profile, and the long loading period means proteins with very high rates of turnover could become fully labelled prior to day 8. The lowest turnover rate measured in the current work (0.32%/d) is greater than the lowest value (0.08%/d) in our previous study [4] so our current data may not represent the full range of protein turnover rates in human muscle. As a general rule, 5 half-lives is considered complete (i.e. 97.5%) when using an exponential model (e.g. Equation 2). Theoretically, if precursor enrichment had been at the steadystate level throughout day 0 to day 8 then a protein with a half-life of 1.6 days (equivalent to turnover rate of 43.3%/d) would be completely labelled by day 8 of the experiment. However, this was not the case in the current experiment and our protocol of incremental deuterium oxide consumption over the first 5 days means higher turnover rate proteins were unlikely to be fully labelled prior to the day 8–12 experimental period.

Conclusion

In summary, the units chosen for reporting protein turnover data affect the biological interpretation of dynamic proteome profiling studies. MTR data is preferred over FTR, particularly for studies on multiprotein complexes, wherein MTR takes account of potential differences amongst the molecular weight of the component subunits. ATR data may be preferred over MTR and FTR, when the aim is to compare between samples that exhibit different abundance profiles. Whereas co-analysis of separate abundance and FTR data is preferred in conditions where proteins exhibit changes in both turnover rate and abundance profile. Protein abundance and other physiochemical characteristics do not predict FTR. Therefore, co-analysis of the abundance and turnover rates of proteins in human muscle is required for correct insight and interpretation.

Supplementary Information

The online version contains supplementary material available at https://doi.org/10.1186/s44330-025-00026-7.

Supplementary Material 1.

Authors' contributions

Conceptualization, P.J.L. and J.G.B.; methodology, J.S.B., S.B., J.P., J.A.S., G.L.C. and J.G.B; formal analysis, B.N.S., J.S.B., S.B., C.A.S., J.P. and J.B.L.; investigation, S.O.S., J.A.S., J.B.L., G.L.C. and P.J.L; resources, G.L.C and J.G.B.; data curation, C.A.S and J.G.B.; writing—original draft preparation, B.N.S., C.A.S. and J.G.B; writing—review and editing, J.S.B. S.B. J.P., S.O.S., J.A.S., J.B.L., G.L.C., and P.J.L.; visualization, B.N.S and C.A.S.; supervision, J.P., S.O.S., J.A.S., J.B.L. and J.G.B.; project administration, J.G.B.; funding acquisition, G.L.C., P.L.J. and J.G.B. All authors have read and agreed to the published version of the manuscript.

Institutional review board statement

The study was approved by the Liverpool John Moores School of Sport and Exercise Science Research Committee (M18SPS006) and conformed with the Declaration of Helsinki, except registration in a publicly accessible database.

Funding

This research received no external funding.

Data availability

The data presented in this study are available in Suppl Table S1 and the raw mass spectrometry files are deposited in ProteomeXchange, PXD046509.

Declarations

Ethics approval and consent to participate
Three physically active males were recruited and received verbal and written information, including potential risks, prior to providing written informed consent. The study was approved by the Liverpool John Moores School of Sport and Exercise Science Research Committee (M18SPS006) and conformed with the Declaration of Helsinki, except registration in a publicly accessible database. Recruitment of participants began in December 2017 and the collection of data and samples from participants was completed by April 2018.

Consent for publication
Not applicable.

Competing interests
The authors declare no competing interests.

Author details
[1]Research Institute for Sport & Exercise Sciences, Liverpool John Moores University, Liverpool L3 3 AF, UK. [2]Department of Applied Mathematics, Liverpool John Moores University, Liverpool L3 3 AF, UK. [3]Present Address: Department of Pharmacology and Toxicology, College of Pharmacy, University of Arizona, Arizona, USA. [4]Present Address: Centre for Systems Health and Integrated Metabolic Research, Department of Biosciences, School of Science and Technology, Nottingham Trent University, Nottingham, UK.

Received: 9 July 2024 Accepted: 27 March 2025
Published online: 14 May 2025

References

1. Li R, Xia J, Zhang X, Gathirua-Mwangi WG, Guo J, Li Y, McKenzie S, Song Y. Associations of Muscle Mass and Strength with All-Cause Mortality among US Older Adults. Med Sci Sports Exerc. 2018;50(3):458–67.
2. Srisawat K, Stead CA, Hesketh K, Pogson M, Strauss JA, Cocks M, Siekmann I, Phillips SM, Lisboa PJ, Shepherd S, et al. People with obesity exhibit losses in muscle proteostasis that are partly improved by exercise training. Proteomics. 2023;24(14):e2300395.
3. O'Reilly CL, Bodine SC, Miller BF. Current limitations and future opportunities of tracer studies of muscle ageing. J Physiol. 2023;603(1):7–15.
4. Camera DM, Burniston JG, Pogson MA, Smiles WJ, Hawley JA. Dynamic proteome profiling of individual proteins in human skeletal muscle after a high-fat diet and resistance exercise. FASEB J. 2017;31(12):5478–94.
5. Schoenheimer R, Ratner S, Rittenberg D. Studies in Protein Metabolism X. The Metabolic Activity of Body Proteins Investigated with l(-)Leucine Containing Two Isotopes. J Biol Chem. 1939;130(2):703–32.
6. Wagenmakers AJM. Tracers to investigate protein and amino acid metabolism in human subjects. Proceedings of the Nutrition Society. 1999;58(4):987–1000.
7. Pratt JM, Petty J, Riba-Garcia I, Robertson DHL, Gaskell SJ, Oliver SG, Beynon RJ. Dynamics of protein turnover, a missing dimension in proteomics. Molecular & cellular proteomics : MCP. 2002;1(8):579–91.
8. Ong SE, Blagoev B, Kratchmarova I, Kristensen DB, Steen H, Pandey A, Mann M. Stable isotope labeling by amino acids in cell culture, SILAC, as a simple and accurate approach to expression proteomics. Molecular & cellular proteomics : MCP. 2002;1(5):376–86.
9. Doherty MK, Hammond DE, Clague MJ, Gaskell SJ, Beynon RJ. Turnover of the human proteome: Determination of protein intracellular stability by dynamic SILAC. J Proteome Res. 2009;8(1):104–12.
10. Cambridge SB, Gnad F, Nguyen C, Bermejo JL, Kruger M, Mann M. Systems-wide proteomic analysis in mammalian cells reveals conserved, functional protein turnover. J Proteome Res. 2011;10(12):5275–84.
11. Rahman M, Sadygov RG. Predicting the protein half-life in tissue from its cellular properties. PLoS ONE. 2017;12(7):1–15.
12. Burniston JG: Investigating Muscle Protein Turnover on a Protein-by-Protein Basis Using Dynamic Proteome Profiling. In: Omics Approaches to Understanding Muscle Biology. Edited by Burniston JG, Chen Y-w, 1 edn. New York: Springer; 2019:171–190.
13. Price JC, Holmes WE, Li KW, Floreani NA, Neese RA, Turner SM, Hellerstein MK. Measurement of human plasma proteome dynamics with2H2O and liquid chromatography tandem mass spectrometry. Anal Biochem. 2012;420(1):73–83.
14. Wang D, Liem DA, Lau E, Ng DC, Bleakley BJ, Cadeiras M, Deng MC, Lam MP, Ping P. Characterization of human plasma proteome dynamics using deuterium oxide. Proteomics Clin Appl. 2014;8(7–8):610–9.
15. Price JC, Khambatta CF, Li KW, Bruss MD, Shankaran M, Dalidd M, Floreani NA, Roberts LS, Turner SM, Holmes WE, et al. The Effect of Long Term Calorie Restriction on in Vivo Hepatic Proteostatis: A Novel Combination of Dynamic and Quantitative Proteomics. Mol Cell Proteomics. 2012;11(12):1801–14.
16. Deberneh HM, Abdelrahman DR, Verma SK, Linares JJ, Murton AJ, Russell WK, Kuyumcu-Martinez MN, Miller BF, Sadygov RG. A large-scale LC-MS dataset of murine liver proteome from time course of heavy water metabolic labeling. Sci Data. 2023;10(1):635.
17. Lau E, Cao Q, Ng DCM, Bleakley BJ, Dincer TU, Bot BM, Wang D, Liem DA, Lam MPY, Ge J, et al. A large dataset of protein dynamics in the mammalian heart proteome. Scientific Data. 2016;3:1–15.
18. Lam MPY, Wang D, Lau E, Liem DA, Kim AK, Ng DCM, Liang X, Bleakley BJ, Liu C, Tabaraki JD, et al. Protein kinetic signatures of the remodeling heart following isoproterenol stimulation. J Clin Investig. 2014;124(4):1734–44.
19. Hesketh SJ, Sutherland H, Lisboa PJ, Jarvis JC, Burniston JG. Adaptation of rat fast-twitch muscle to endurance activity is underpinned by changes to protein degradation as well as protein synthesis. FASEB journal : official publication of the Federation of American Societies for Experimental Biology. 2020;34(8):10398–417.
20. Shankaran M, Shearer TW, Stimpson SA, Turner SM, King C, Wong PYA, Shen Y, Turnbull PS, Kramer F, Clifton L, et al. Proteome-wide muscle protein fractional synthesis rates predict muscle mass gain in response to a selective androgen receptor modulator in rats. American Journal of Physiology - Endocrinology and Metabolism. 2016;310(6):E405–17.
21. Scalzo RL, Peltonen GL, Binns SE, Shankaran M, Giordano GR, Hartley DA, Klochak AL, Lonac MC, Paris HLR, Szallar SE, et al. Greater muscle protein synthesis and mitochondrial biogenesis in males compared with females during sprint interval training. FASEB J. 2014;28(6):2705–14.
22. Shankaran M, King CL, Angel TE, Holmes WE, Li KW, Colangelo M, Price JC, Turner SM, Bell C, Hamilton KL, et al. Circulating protein synthesis rates reveal skeletal muscle proteome dynamics. J Clin Investig. 2016;126(1):288–302.
23. Murphy CH, Shankaran M, Churchward-Venne TA, Mitchell CJ, Kolar NM, Burke LM, Hawley JA, Kassis A, Karagounis LG, Li K et al: Effect of resistance training and protein intake pattern on myofibrillar protein synthesis and proteome kinetics in older men in energy restriction. In: Journal of Physiology. 2018;11:2091–2120.
24. Srisawat K, Hesketh K, Cocks M, Strauss J, Edwards BJ, Lisboa PJ, Shepherd S, Burniston JG. Reliability of Protein Abundance and Synthesis Measurements in Human Skeletal Muscle. Proteomics. 2019;1900194:1900194–1900194.
25. Robinson MM, Dasari S, Konopka AR, Johnson ML, Manjunatha S, Esponda RR, Carter RE, Lanza IR, Nair KS. Enhanced Protein Translation Underlies Improved Metabolic and Physical Adaptations to Different Exercise Training Modes in Young and Old Humans. Cell Metab. 2017;25(3):581–92.
26. Murgia M, Toniolo L, Nagaraj N, Ciciliot S, Vindigni V, Schiaffino S, Reggiani C, Mann M. Single Muscle Fiber Proteomics Reveals Fiber-Type-Specific Features of Human Muscle Aging. Cell Rep. 2017;19(11):2396–409.
27. Ubaida-Mohien C, Lyashkov A, Gonzalez-Freire M, Tharakan R, Shardell M, Moaddel R, Semba RD, Chia CW, Gorospe M, Sen R, et al. Discovery proteomics in aging human skeletal muscle finds change in spliceosome, immunity, proteostasis and mitochondria. Life. 2019;8:1–27.
28. Öhman T, Teppo J, Datta N, Mäkinen S, Varjosalo M, Koistinen HA. Skeletal muscle proteomes reveal downregulation of mitochondrial proteins in transition from prediabetes into type 2 diabetes. Science. 2021;24(7):102712–102712.
29. Kobak KA, Lawrence MM, Pharaoh G, Borowik AK, Iii FFP, Miller BF, Shipman PD, Grif TM, Remmen HV. Determining the contributions of protein synthesis and breakdown to muscle atrophy requires non-steady-state equations. 2021;12(6):1764–75.

30. Stansfield BN, Brown AD, Stewart CE, Burniston JG: Dynamic Profiling of Protein Mole Synthesis Rates During C2C12 Myoblast Differentiation. Proteomics 2020:e2000071-e2000071.
31. Silva JC, Gorenstein MV. Li G-z, Vissers JPC, Geromanos SJ: Absolute Quantification of Proteins by LCMS E. Mol Cell Proteomics. 2006;5(1):144–56.
32. Wiśniewski JR, Hein MY, Cox J, Mann M. A "proteomic ruler" for protein copy number and concentration estimation without spike-in standards. Mol Cell Proteomics. 2014;13(12):3497–506.
33. Bennett S, Tiollier E, Brocherie F, Owens DJ, Morton JP, Louis J. Three weeks of a home-based "sleep low-train low" intervention improves functional threshold power in trained cyclists: A feasibility study. PLoS ONE. 2021;16(12): e0260959.
34. McCabe BJ, Bederman IR, Croniger C, Millward C, Norment C, Previs SF. Reproducibility of gas chromatography-mass spectrometry measurements of2H labeling of water: Application for measuring body composition in mice. Anal Biochem. 2006;350(2):171–6.
35. Wisniewski JR, Zougman A, Nagaraj N, Mann M, Wi JR. Universal sample preparation method for proteome analysis. Nat Methods. 2009;6(5):377–362.
36. Sadygov RG. Protein turnover models for LC-MS data of heavy water metabolic labeling. Brief Bioinform. 2022;23(2):bbab598. PMID: 35062023.
37. Holmes WE, Angel TE, Li KW, Hellerstein MK: Dynamic Proteomics: In Vivo Proteome-Wide Measurement of Protein Kinetics Using Metabolic Labeling. Methods Enzymol. 2015;561:219–276.
38. Kanehisa M, Goto S. KEGG: kyoto encyclopedia of genes and genomes. Nucleic Acids Res. 2000;28(1):27–30.
39. Tyanova S, Temu T, Sinitcyn P, Carlson A, Hein MY, Geiger T, Mann M, Cox J. The Perseus computational platform for comprehensive analysis of (prote)omics data. Nat Methods. 2016;13(9):731–40.
40. Franceschini A, Szklarczyk D, Frankild S, Kuhn M, Simonovic M, Roth A, Lin J, Minguez P, Bork P, Von Mering C, et al. STRING v9.1: Protein-protein interaction networks, with increased coverage and integration. Nucleic Acids Res. 2013;41(D1):808–15.
41. Storey JD, Tibshirani R. Statistical significance for genomewide studies. Proc Natl Acad Sci USA. 2003;100(16):9440–5.
42. Meldal BHM, Forner-Martinez O, Costanzo MC, Dana J, Demeter J, Dumousseau M, Dwight SS, Gaulton A, Licata L, Melidoni AN, et al. The complex portal - An encyclopaedia of macromolecular complexes. Nucleic Acids Res. 2015;43(D1):D479–84.
43. Stead CA, Hesketh SJ, Bennett S, Sutherland H, Jarvis JC, Lisboa PJ, Burniston JG. Fractional synthesis rates of individual proteins in rat soleus and plantaris muscles. Proteomes. 2020;8(2):10–10.
44. Brook MS, Wilkinson DJ, Mitchell WK, Lund JN, Phillips BE, Szewczyk NJ, Greenhaff PL, Smith K, Atherton PJ. Synchronous deficits in cumulative muscle protein synthesis and ribosomal biogenesis underlie age-related anabolic resistance to exercise in humans. J Physiol. 2016;594(24):7399–417.
45. Martin-Perez M, Villén J. Determinants and Regulation of Protein Turnover in Yeast. Cell Syst. 2017;5(3):283-294.e285.
46. Gonzalez-Franquesa A, Stocks B, Chubanava S, Hattel HB, Moreno-Justicia R, Treebak JT, Zierath JR, Deshmukh AS. Mass-spectrometry based proteomics reveals mitochondrial supercomplexome plasticity. 2021;35(8):109180.
47. Acín-Pérez R, Fernández-Silva P, Peleato ML, Pérez-Martos A, Enriquez JA. Respiratory Active Mitochondrial Supercomplexes. Mol Cell. 2008;32(4):529–39.
48. Ubaida-Mohien C, Gonzalez-Freire M, Lyashkov A, Moaddel R, Chia CW, Simonsick EM, Sen R, Ferrucci L. Physical activity associated proteomics of skeletal muscle: Being proteomics of skeletal muscle: Being physically active in daily life may protect skeletal muscle from aging. Frontiers in Physiology. 2019;10(MAR):1–16.
49. Greggio C, Jha P, Kulkarni SS, Lagarrigue S, Broskey NT, Boutant M, Wang X, Conde Alonso S, Ofori E, Auwerx J, et al. Enhanced Respiratory Chain Supercomplex Formation in Response to Exercise in Human Skeletal Muscle. Cell Metab. 2017;25(2):301–11.
50. Saraste M. Oxidative phosphorylation at the fin de siecle. Science. 1999;283(5407):1488–93.
51. DiMauro S, Schon EA. Mitochondrial DNA mutations in human disease. Am J Med Genet. 2001;106(1):18–26.
52. Burniston JG, Hoffman EP. Proteomic responses of skeletal and cardiac muscle to exercise. Expert Rev Proteomics. 2011;8(3):361–77.
53. Kucharczyk R, Ezkurdia N, Couplan E, Procaccio V, Ackerman SH, Blondel M, di Rago JP. Consequences of the pathogenic T9176C mutation of human mitochondrial DNA on yeast mitochondrial ATP synthase. Biochim Biophys Acta. 2010;1797(6–7):1105–12.
54. Boisvert FM, Ahmad Y, Gierliński M, Charrière F, Lamont D, Scott M, Barton G, Lamond AI. A quantitative spatial proteomics analysis of proteome turnover in human cells. Mol Cell Proteomics. 2012;11(3):1–15.
55. Zecha J, Meng C, Zolg DP, Samaras P, Wilhelm M, Kuster B. Peptide level turnover measurements enable the study of proteoform dynamics. Mol Cell Proteomics. 2018;17(5):974–92.
56. Holloway KV, Gorman MO, Woods P, Morton JP, Evans L, Cable NT, Goldspink DF, Burniston JG. Proteomic investigation of changes in human vastus lateralis muscle in response to interval-exercise training. Proteomics. 2009;9(22):5155–74.
57. Hesketh S, Srisawat K, Sutherland H, Jarvis JC, Burniston JG. On the Rate of Synthesis of Individual Proteins within and between Different Striated Muscles of the Rat. Proteomes. 2016;4(1):12–12.
58. Fuqua JD, Lawrence MM, Hettinger ZR, Borowik AK, Brecheen PL, Szczygiel MM, Abbott CB, Peelor FF 3rd, Confides AL, Kinter M, et al. Impaired proteostatic mechanisms other than decreased protein synthesis limit old skeletal muscle recovery after disuse atrophy. J Cachexia Sarcopenia Muscle. 2023;14(5):2076–89.
59. Jones PJ, Leatherdale ST. Stable isotopes in clinical research: safety reaffirmed. Clin Sci (Lond). 1991;80(4):277–80.

Publisher's Note